 doi:10.20944/preprints202205.0055.v1

Article

High Diffusion Permeability of Anion Exchange Membranes for Ammonium Chloride: Experiment and Modeling

Ekaterina Skolotneva, Ksenia Tsygurina, Semyon Mareev, Ekaterina Melnikova, Natalia Pismenskaya and Victor Nikonenko*

Membrane Institute, Kuban State University, 149 Stavropolskaya st., 350040 Krasnodar, Russia; mareev-semyon@bk.ru (S.M.); kseniya_alx@mail.ru (K, T.); ek.skolotneva@gmail.com (E.S.); n_pismen@mail.ru (N. P.)

* Correspondence: v_nikonenko@mail.ru; Tel.: +7-918-414-5816

Abstract: It is known that ammonium has a higher permeability through anion-exchange and bipolar membranes compared to K^+ cation that has the same mobility in water. However, the mechanism of this high permeability is not clear enough. We develop a mathematical model based of the Nernst-Planck and Poisson equations for diffusion of ammonium chloride through an anion-exchange membrane; proton exchange reactions between ammonium, water and ammonia are taken into account. It is assumed that ammonium, chloride and OH^- ions can only pass through membrane hydrophilic pores, while ammonia can also dissolve in membrane matrix fragments not containing water and diffuse through these fragments. It is found that due to the Donnan exclusion of H+ ions as coions, the pH in the membrane internal solution increases when approaching the membrane side facing distilled water. Consequently, there is a change in the principal nitrogen-atom carrier in the membrane: in the part close to the side facing the feed NH_4Cl solution (pH<8.8), it is the NH_4^+ cation, and in the part close to distilled water, NH_3 molecules. The concentration of NH_4^+ reaches almost zero at a point close to the middle of the membrane cross-section, which approximately halves the effective thickness of the diffusion layer for the transport of this ion. When NH_3 takes over the nitrogen transport, it only needs to pass through the other half of the membrane. Leaving the membrane, it captures an H+ ion from water, and the released OH^- goes towards the membrane side facing the feed solution to meet the NH_4^+ ions. The comparison of the simulation with experiment shows a satisfactory agreement.

Keywords: ion exchange membrane, diffusion permeability, weak electrolyte, ammonium chloride, simulation.

1. Introduction

Nitrogen extraction from the wastewaters is crucial for achieving the sustainable development goals. The presence of nitrogen in wastewater causes significant harm to the environment. Nitrogen removal can prevent the waters from eutrophication [1], leading to the degradation of water quality, an enlarged emissions of N_2O (which is the greenhouse gas and has the highest impact on ozone depletion among other ozone-depleting gazes [2]) produced by bacteria into the atmosphere [3] and the occurrence of harmful algae blooms [4]. On the other hand, the ammonia nitrogen is a key component of fertilizers [5], which are needed more and more to produce enough rations to feed the growing global population and overcome hunger [6]. Nowadays ammonia is synthesized commercially using Haber-Bosch process, which is a highly energy intensive technology [7]. There are statistical data [8,9] predicting the 1-2% of world energy consumption spent on Haber-Bosch process in the coming years. At the same time, only 16% of nitrogen from fertilizers is absorbed by animals or humans, and the rest is released into the atmosphere or hydrosphere. Therefore, the ammonia recuperation from wastewater is a promising source of

Preprints (www.preprints.org) | NOT PEER-REVIEWED | Posted: 5 May 2022 doi:10.20944/preprints202205.0055.v1

ammonia. In addition, ammonia salts have significant application potential for carbon-free energy storage and electrical power generation [10–13].

To the date, the various methods of ammonia extraction are established (chemical precipitation/crystallization, liquid-gas stripping) or intensively developed (adsorption, bioelectrochemical methods and electrodialysis (ED)) [14,15]. Among these technologies, ED stands out among others as it allows obtaining commercially attractive concentrates using feed solutions with low concentration [16–18]. However, by its chemical nature, ammonium is an ampholyte, i.e., it participates in protonation-deprotonation reactions and can change its structure and charge depending on the pH value (Figure 1). Thus, its behavior in the electromembrane systems is more complicated and less predictable than that of strong electrolyte solutions such as NaCl, KCl, $NaNO_3$ etc.

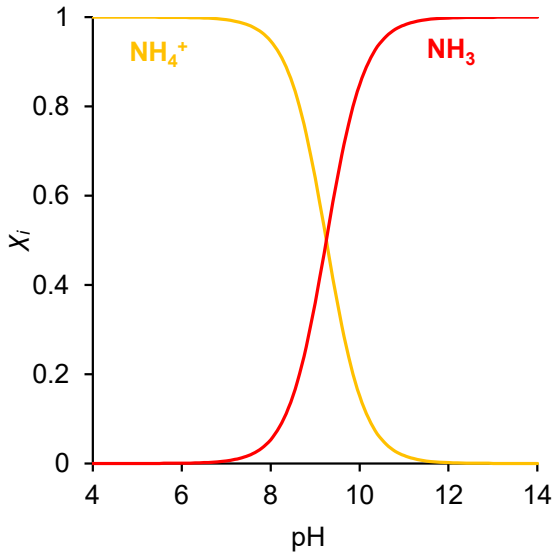

Figure 1. The molar fraction (χi) of the components of an aqueous solution of NH4Cl as a function of pH.

There is a number of studies pointing to the increased water splitting at anion exchange membranes (AEMs) in ammonia-containing solutions [19–22]; in addition, the AEM permeability for ammonium ions is found higher than for other anions [22,23]. The results of these studies allow us to suggest that the specific behavior of AEMs in ammonium-containing solutions is due to protonation-deprotonation reactions involving nitrogen ammonia species, which are coupled with a pH shift in these membranes in relation to the pH of the external solution. The latter is caused by the Donnan exclusion of protons as coions from AEMs [24]. This assumption is confirmed by the fact that in systems with bipolar membranes, inside which the pH shift is even more significant than in systems with monopolar membranes, the diffusion of ammonium through the anion-exchange layer is even more considerable [25–27].

It should also note that ammonia molecules are very similar in their properties to water molecules. Indeed, both molecules have the same molecular orbital hybridization, both are polar and have close values of size (2.60 Å for ammonia and 2.65 Å for water) and dipole moment (1.47 D for ammonia and 1.85 D for water [28]), both are able to form hydrogen bonds. This resemblance leads to the fact that ammonia can penetrate through biological membranes, which are selective to water transport [29–31]. Moreover, there are studies showing that in ammonia media the same specific mechanism of proton transfer as in water is possible. Grotthus-type proton hops along an "ammonia wire" involving NH_3 molecules are proved in [32,33].

Despite the experimental evidence of unusual behavior of systems with ammonia-containing solutions, there are very few theoretical studies in this field. In the previous

Preprints (www.preprints.org) | NOT PEER-REVIEWED | Posted: 5 May 2022 doi:10.20944/preprints202205.0055.v1

work of our group [34], the high ammonium transport through the AEM is explained by a mechanism similar to the facilitated diffusion, or carrier-mediated diffusion of various substances, e.g. amino acids, which is widely described in the literature [35–38]. It is established that due to the Donnan exclusion of H^+ ions the pH inside the AEM increases [24]. Therefore, when the NH_4^+ ions being coions for an AEM enter the membrane, a part of them loses their charge and is transformed into NH_3 molecules, which are not excluded from the membrane. Therefore, nitrogen transfer through an AEM is possible not only with NH_4^+ ions, but it can also be carried by NH_3 molecules. For the examination of this hypothesis, a one-dimensional stationary mathematical model of ammonium chloride transport through AEM was developed on the base of the Nernst-Planck equation and the local electroneutrality assumption; protonation-deprotonation reactions inside the membrane were taken into account. The conditions of local ion-exchange equilibrium at the solution/membrane interfaces and chemical equilibrium at any point were assumed. The latter implies that the rate constants of the protonation-deprotonation reactions are infinitely large. A qualitative agreement between the experimental data and the results of simulation was found.

A similar mechanism of ammonium transfer, taking into account protonation-deprotonation reactions, but through a cation-exchange membrane (CEM), is studied experimentally and theoretically by Liu et al. [39]. During the experiment it was found that the ammonium concentration in the anode chamber decreased due to its transfer through the CEM to the cathode chamber, but the ammonium concentration in the cathode chamber remained almost constant and close to zero. The suggested explanation of this phenomena was the deprotonation of ammonium ions and their transformation in the ammonia molecules in the cathode chamber where a high value of pH is due to OH^- generation on this electrode. However, the authors did not observe the back diffusion of nitrogen in the ammonia form into the anode chamber. Mathematical modelling showed that inside the membrane pH increases from an acidic value at the interface with the anolyte (where H^+ ions are generated at the anode) to an alkaline value at the interface with the catholyte. Therefore, ammonia molecules, passing through the membrane and entering its acidic region, are protonated and turned into the ammonia ions, which are transferred back to the cathode chamber. Using the mathematical model, the authors also showed that at low and medium values of electric current, the diffusion of ammonium through the CEM prevails over migration. The assumptions made in the model were similar to those used in Ref. [33]; in particular, the conditions of local electrical neutrality and chemical equilibrium were accepted.

The purpose of this work is to clarify the reasons for the high diffusion permeability of AEMs in an ammonium chloride solution. We present experimental data and a novel 1D stationary mathematical model of the weak electrolyte transport in membrane system to explain the phenomenon. As in the previous theoretical works [34,39], the Nernst-Planck equations are used with taking into account the protonation-deprotonations reactions between NH_4^+ and NH_3. However, instead of the local electroneutrality assumption, we use the Poisson equation; instead of chemical equilibrium assumption, we apply equations describing kinetics of chemical reactions with finite rate constants. A new assumption is applied: ammonium, chloride and hydroxyl ions can only pass through the hydrophilic pores of an AEM, while ammonia can diffuse both through the pores and through fragments of the membrane matrix that do not contain water.

2. Results and Discussions

2.1 Diffusion Permeability and Conductivity of IEMs

The integral diffusion permeability coefficient, P, of an ion-exchange membrane is a proportionality factor in the following equation determining the diffusion flux density, j, of dissolved salt through the membrane in conditions where the membrane is bathed by a (feed) solution of concentration c on one side and by distilled water on the other:

Preprints (www.preprints.org) | NOT PEER-REVIEWED | Posted: 5 May 2022 doi:10.20944/preprints202205.0055.v1

$$j = P\frac{c}{d} \quad (1)$$

where d is the membrane thickness. P is found by measuring the value of j for a given value of c (see the Section 3.2 for more details). Instead of difference in concentrations on both sides of the membrane, the numerator contains only the concentration of the feed (bulk) solution, since there is pure water on the other membrane side and the effect of diffusion layers in the solution is assumed to be negligible.

The membrane conductivity, κ, (in S/m) was measured as described in Section 3.3. The results of measurements of P and κ of the membranes under study in KCl and NH_4Cl solutions are presented in Figures 2 and 3.

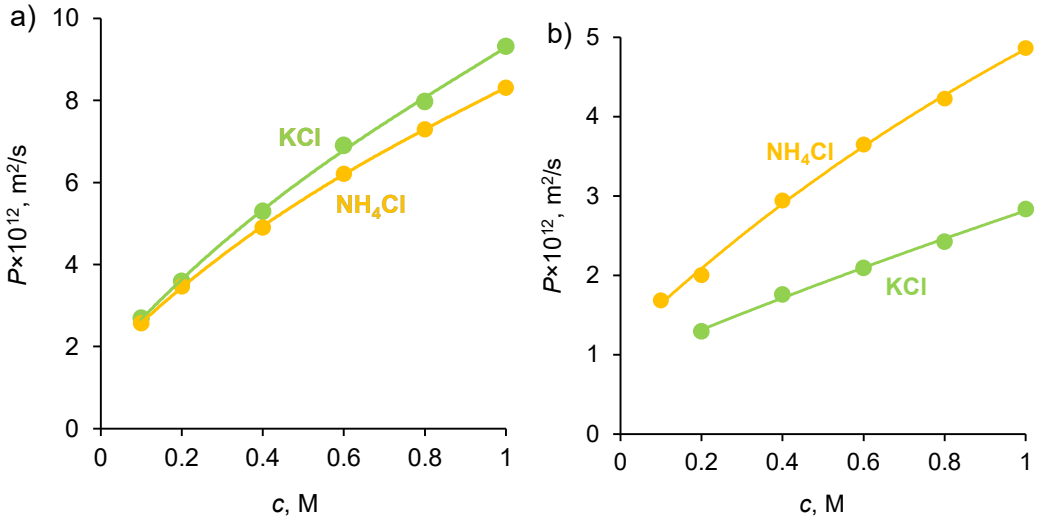

Figure 2. Integral diffusion permeability coefficient of CMX (a) and AMX (b) membranes in KCl and NH_4Cl solutions. The dots are experimental data, the solid lines are given to lead the eye.

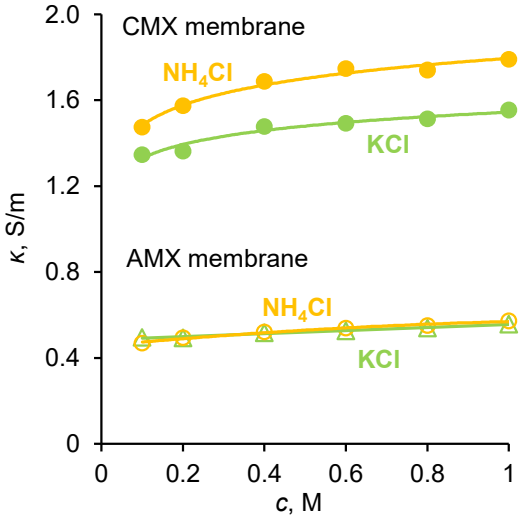

Figure 3. The conductivity of CMX and AMX membranes in KCl and NH_4Cl solutions. The dots correspond to the experimental data, the solid lines are given to lead the eye.

Preprints (www.preprints.org) | NOT PEER-REVIEWED | Posted: 5 May 2022 doi:10.20944/preprints202205.0055.v1

According to theoretical and experimental studies [40–43], the diffusion permeability of AEMs and CEMs is controlled by the transport of coions, while the conductivity is controlled by the transport of counterions. Both quantities increase with increasing the solution concentration, since the concentration of both counterions and coions in the membranes growth as the solution concentration, c, increases. Moreover, the coion concentration in the micropores increases approximately as c^2 [40,44]. As Figure 2a shows, the diffusion permeability of the homogeneous Neosepta cation exchange CMX membrane (Astom Corp., Japan, see more details about properties in Section 3.1) in KCl and NH_4Cl solutions weekly depends on the type of electrolyte, since the coion, Cl^-, is the same in both solutions. Similarly, the conductivity of the homogeneous Neosepta anion-exchange AMX membrane (Astom Corp., Japan) in both electrolytes is very close, sine the counterion is the same.

Note also, that the self-diffusion coefficients of K^+ and NH_4^+ in solution have very close values (1.957×10^{-9} m^2/s in an infinite dilute solution [28,45]). However, the conductivity of CMX in the NH_4^+ form is slightly (by about 15%) greater than that in the K^+ form. Therefore, we can assume that the diffusion coefficient of NH_4^+ in this membrane is slightly greater than that of K^+. This difference could be due to a slightly higher CMX membrane hydration in the presence of NH_4^+ compared to K^+. The reason to think so is in the fact that according to Hua et al. [46], NH_4Cl significantly greater than KCl perturbs water's hydrogen-bonding network. Additionally, the experimental data of Fuoco et al. [47] show that the freezing point of water in the CMX membrane equilibrated with KCl solution is −15.9°C, and with NH_4Cl is −12.8°C. These results allow concluding that in the case of ammonium, the pores are larger and water is less bound, which explains the higher mobility of ammonium ions and the higher conductivity of the membrane in the form of these ions. As for the integral diffusion permeability coefficient of the AMX membrane, it is-almost twice as much if the membrane contacts an NH_4Cl solution, compared to a KCl solution (Figure 2b). The value of P is proportional to the $\overline{D}_2\overline{c}_2$ product, where $\overline{D}_2$ and $\overline{c}_2$ are the diffusion coefficient and concentration of coion (subscript 2), respectively [40,48], see also Section 4.3. We do not see reasons, why the diffusion coefficient and concentration of NH_4^+ ions would be much greater than those of K^+ ions in an AMX membrane. Both cations, due to electrostatic repulsion from the positively charged quaternary ammonium groups (comprising most of the fixed functional groups of the AMX membrane), are not able to approach the fixed groups of the membrane matrix and interact with them. We are more inclined to accept the hypothesis, expressed in the Introduction, that the elevated transfer of nitrogen through an AEM, such as AMX, is due to the contribution of ammonia molecules. These uncharged molecules can approach the fixed charged groups, hence, they can occupy more space in the membrane, so that their concentration can be significant. This hypothesis is supported also by publications [49,50] on the permeability of gas separation membranes. According to these publications, the presence of ammonium salts in the membrane matrix can significantly increase its selectivity with respect to ammonia. This fact has been repeatedly confirmed, on the basis of which a patented method for gas separation have been developed [51]. Study [49] shows that the most probable mechanism of a high ammonia transport is due to its great sorption: ammonia dissolves in ammonium thiocyanate and diffuses across the membrane.

2.2 Mathematical modeling of diffusion permeability of AMX membrane

We describe mathematically the following process. As mentioned in the Introduction, pH of the internal solution in an AEM is higher than the pH of the external solution adjacent to the membrane surface since H^+ ions are expelled from the membrane as coions. Therefore, when NH_4^+ ions enter the membrane under the action of their concentration gradient, some of them are deprotonated and converted into NH_3 molecules (Figure 4). The NH_3 molecules diffuse through the membrane to its boundary with the depleted solution, initially distilled water. When leaving the membrane, they are protonated and

Preprints (www.preprints.org) | NOT PEER-REVIEWED | Posted: 5 May 2022 doi:10.20944/preprints202205.0055.v1

again return to the form of NH_4^+ ions. The released OH^- ions return to membrane boundary contacting with the feed solution. Here these ions take part in the reaction of deprotonation of new NH_4^+ ions entering the membrane.

The 1D steady-state model of diffusion transport of ammonium chloride through an AEM is developed. A three-layer system consisting of an AEM and two adjacent diffusion layers is considered (Figure 4). The membrane is placed between an NH_4Cl solution and distilled water, the diffusion of ions from the solution to the distilled water through the membrane is studied. The Nernst-Planck equations involving ion and molecule activity coefficients coupled with the Poisson equation are applied. In the membrane, the transport of ions is modelled within the pores with charged walls, where the concentrations are considered as averaged over the pore cross-section. Since ions can pass only through the pores, the flux density per square meter of the membrane cross-section is found by multiplying the flux density through the pore (in mol $s^{-1}m^2$ pore cross-section) on the membrane porosity p (assumed equal to 0.3 for AMX, as typical value for membranes made by paste method). However, as mentioned above, ammonia non-charged species can transfer not only inside the pores, but also inside the non-charged fragments of membrane matrix. Therefore, the flux density found for NH_3 species is not multiplied by p.

Ammonia protonation-deprotonation and water dissociation-recombination reactions are taken into account with finite rate constants. Within the solution/membrane interfaces (of the thickness of about 1 nm), we assume the continuity of the activity of all species when passing through the interface between solution and membrane; with that the activity coefficients change continuously from their values in the solution (where they are equal to 1) to their specific values in the membrane. As well, the electric potential changes continuously in the interface. This assures continuity of the electrochemical potential of each species in the interface. The mathematical formulation of the model is described in detail in Section 4 "Mathematical model". The input parameters are discussed below, they are all present in Table 1, Section 4.3.

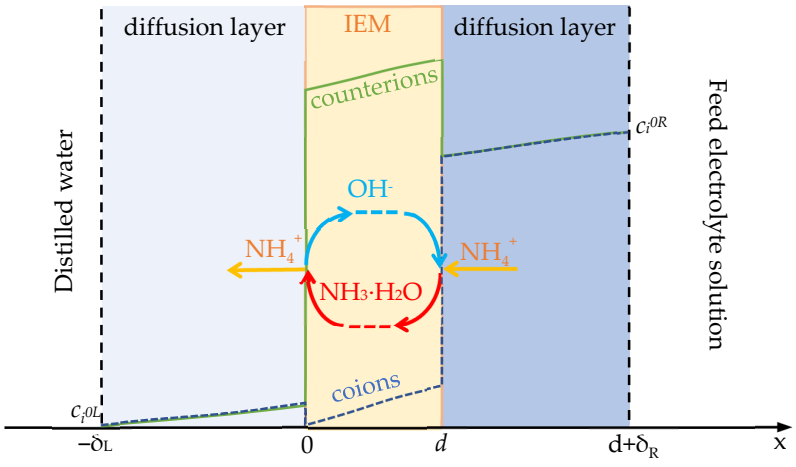

Figure 4. Schematic representation of the system under study. Here δ_L, δ_R and d are diffusion boundary layer (L – left-hand and R – right-hand) and membrane thicknesses, respectively.

The processing of the experimental data and the adjustment of the activity coefficients made it possible to achieve good agreement between the theoretical and experimental data (Figure 5).

Preprints (www.preprints.org) | NOT PEER-REVIEWED | Posted: 5 May 2022 doi:10.20944/preprints202205.0055.v1

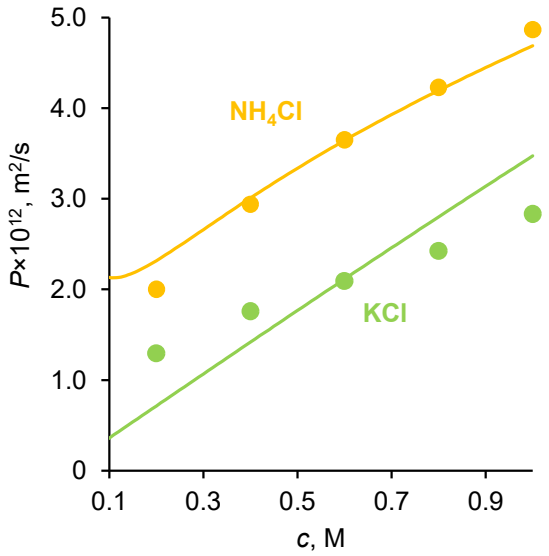

Figure 5. Dependence of the experimental (lines) and theoretical (dots) integral diffusion permeability coefficients of NH_4Cl and KCl on the concentration of the external solution in the membrane system with AMX membrane. The model parameters used in the calculation are presented in Section 4.3 (Table 1).

2.3 Determination of the input parameters

Activity coefficients in solution are taken the same and equal to 1 for all species. Activity coefficients in the membrane are selected taken into account affinity of the membrane for some specific species. As mentioned in the Section 2.1, NH_3 can be absorbed not only within the pores, but within the membrane matrix not containing water also [49]. The continuity activity condition at the interfaces used in the model, assume that for a species i (on the left side of the membrane)

$$a_i(0-,t) = a_i(0+,t) \tag{2}$$

It follows from Equation (2) and definition $a_i = c_i\gamma_i$, that

$$c_i(0+,t) = c_i(0-,t)\gamma_i / \overline{\gamma}_i \tag{3}$$

where $\gamma_i / \overline{\gamma}_i = K_s$ is the partition coefficient, the overbar means that the value refers to the membrane phase. We use the value $\overline{\gamma}_{NH_3}$=0.03, which gives K_s=33 for ammonia molecules. Similarly, the value of $\overline{\gamma}_{OH^-}$ is assumed to be 0.02, since it is known that the pH of the internal solution of the AMX membrane is quite elevated and reach about 10–11 according to the measurements by using a color indicator (anthocyanin), when the external solution is 0.02 M NH_4Cl or KCl [22].

Diffusion coefficients in the membrane. The model of a homogeneous membrane used in this work (similar to the Teorell, Meyer and Sievers (TMS) model [40]) describes quantitatively the properties of the membrane only in a small range of the external solution concentration (up to 0.2 M). To describe the properties of the system in a wider range of concentrations, effective diffusion coefficients, which depend on the concentration of the external solution, should be used. Theoretically, the dependence of effective diffusion coefficients on concentration can be taken into account if a model, which takes into account the heterogeneous structure of the membrane (for example, the microheterogeneous model [52]), is applied. However, the use of such a model would significantly increase the mathematical difficulties and complicate the understanding of the reasons for the high diffusion permeability of AEMs for NH_4Cl. In this paper, of greatest interest is the con-

Preprints (www.preprints.org) | NOT PEER-REVIEWED | Posted: 5 May 2022 doi:10.20944/preprints202205.0055.v1

centration range (0.5–1.0 M), in which electrodialysis concentration or conversion of ammonium-containing solutions usually occurs. Therefore, we will focus on this range of concentrations.

For the CMX membrane, the K^+ and NH_4^+ ions are counterions, inside the membrane they are electrostatically attracted by fixed groups, which, at a distance less than the Bjerrum length, leads to possible specific interactions [53]. Figure 3 shows that the electrical conductivity of CMX in KCl and NH_4Cl solutions differs by no more than 15%. This means that the diffusion coefficients of K^+ and NH_4^+ in the cation-exchange membrane can differ by no more than 15%. Calculations according to Equation (30) in Section 4.3 gives the diffusion coefficients of K^+ and NH_4^+ in the CMX membrane equal to 5.2×10^{-11} m²/s and 6.0×10^{-11} m²/s, respectively (at a feed solution concentration of 0.4 – 1 M). In the case of an anion-exchange membrane, the K^+ and NH_4^+ ions are coions. Inside an AEM, they are electrostatically repelled by fixed groups. The difference between the diffusion coefficients of K^+ and NH_4^+ inside the anion-exchange membrane should also not be large, since their diffusion coefficients are the same in a free solution. Based on the foregoing, we can assume that the diffusion coefficients of K^+ and NH_4^+ in AEM are approximately the same.

Calculations show that a change in the activity coefficients of H^+ and OH^- ions in the range from 0.02 to 10 in the case of a KCl solution does not significantly affect the value of the KCl diffusion flux through the AEM. This flux at the feed solution concentration 1 M is 2.22×10^{-5} mol/(m²s), which corresponds to $P=2.8\times10^{-12}$ m²/s and is in a good agreement with experiment (Figures 5). The deviation in the calculated values of the flux when varying the values $\overline{\gamma}_{OH^-}$ and $\overline{\gamma}_{H^+}$ does not exceed 0.1%. In other words, a change in the activity coefficients $\overline{\gamma}_{OH^-}$ and $\overline{\gamma}_{H^+}$ should not lead to a change in the KCl diffusion flux through the membrane, since the presence/absence of OH^- and H^+ ions does not affect the equilibrium of the potassium chloride dissociation reaction, and, as a result, its flux. Really, KCl is a strong electrolyte: in the studied pH and concentrations ranges it almost completely dissociates into K^+ and Cl^- ions in aqueous solutions.

Figure 6 shows the concentration profiles of the components of an aqueous solution of KCl in AEM and in adjacent diffusion layers. Inside the membrane, at the boundary with the feed electrolyte solution, the concentrations of K^+ and Cl^- ions take the maximum values: the concentration of counterions Cl^- is close to the ion exchange capacity of AEM, and the concentration of coions is many times lower due to the Donnan (electrostatic) exclusion of coions. As it is known [40], this effect is enhanced with dilution of the external solution. Therefore, at the side of the AOM adjoining the dilute solution (initially distilled water), an even more significant decrease in the concentration of coions (K^+ and H^+) in the membrane is observed, at least by three orders of magnitude compared to Cl^- anions. Due to the low concentration of H^+ coions at the boundary with a dilute solution, the concentration of OH^- ions at this boundary reaches its highest value in the membrane, which increases with decreasing $\overline{\gamma}_{OH^-}$ and reaches 2×10^{-5} M (pH=9.9) at $\overline{\gamma}_{OH^-}$=0.03.

The fact that the flux of KCl through an AEM does not depend on $\overline{\gamma}_{OH^-}$, reduces the number of influencing parameters on the results of simulation of KCl diffusion through the AMX membrane and allows fitting the diffusion coefficient of K^+ in this membrane, which gives $\overline{D}_{K^+}=2.7\times10^{-11}$ m²/s. As follows from the above analysis, the diffusion coefficient of NH_4^+ in this membrane should be very close to that of K^+. Therefore, we find $\overline{D}_{NH_4^+}=\overline{D}_{K^+}=2.7\times10^{-11}$ m²/s.

The diffusion coefficients of OH^-, H^+ and NH_3 in the membrane are selected to be relatively high, only three times lower than the corresponding values in solution (Table 1), – to match the high fluxes of NH_4Cl through the AMX membrane, found experimentally. Fitting of $\overline{\gamma}_{OH^-}$ and $\overline{\gamma}_{NH_3}$ makes it possible to achieve good agreement between the experimental and theoretical dependences of the diffusion permeability coefficient of the AMX membrane for NH_4Cl. The best agreement is reached with $\overline{\gamma}_{OH^-}=0.03$ and $\overline{\gamma}_{NH_3}=0.03$.

Preprints (www.preprints.org) | NOT PEER-REVIEWED | Posted: 5 May 2022 doi:10.20944/preprints202205.0055.v1

Further details of the determination of diffusion coefficients in the membranes are given in Section 4.3.

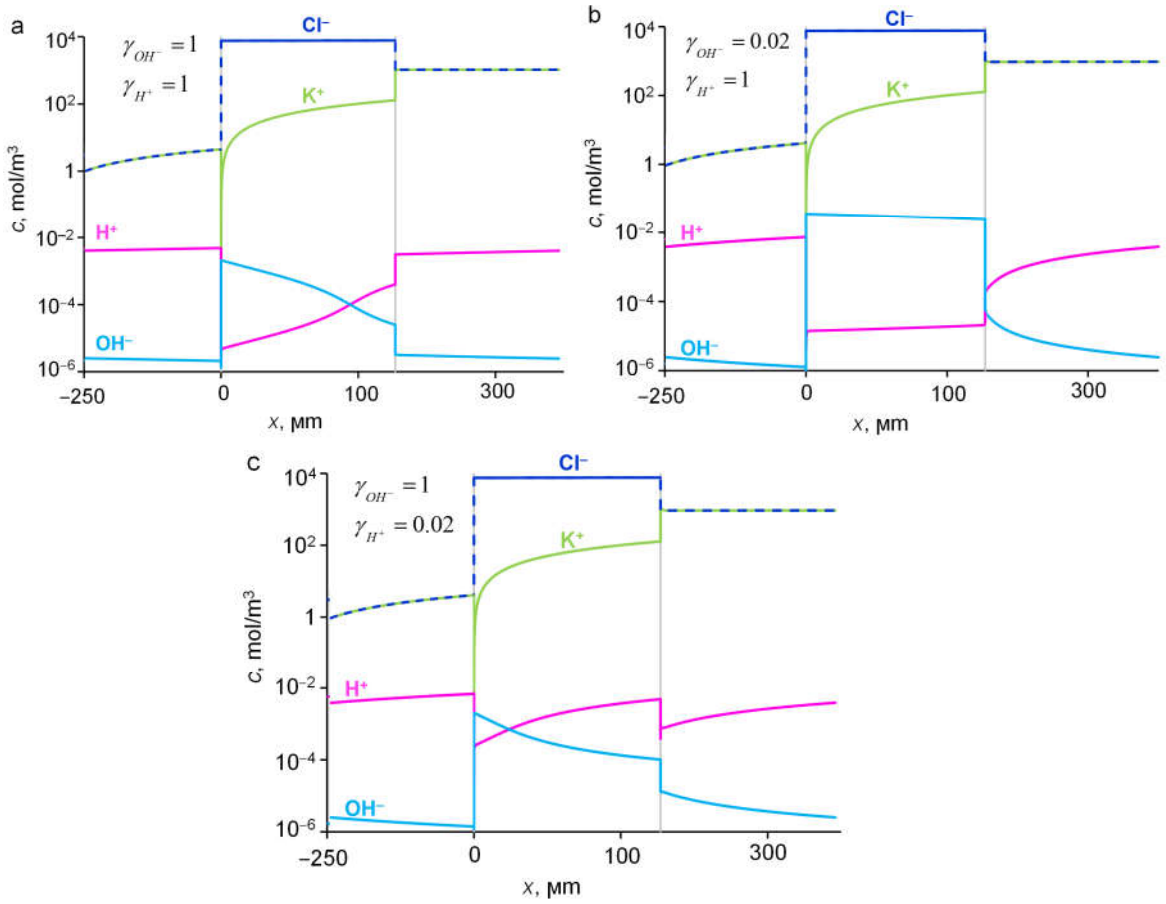

Figure 6. Distribution of ion concentrations in the system under study at different $\overline{\gamma}_{OH^-}$ and $\overline{\gamma}_{H^+}$ (indicated in the plots) at 1M of feed electrolyte KCl solution. Simulation with the input parameters presented in Table 1.

2.4 Concentrations and fluxes in the case of NH₄Cl

Figure 7 shows the distribution of concentrations of all species present in aqueous NH_4Cl solution when ammonium chloride diffuses through an AEM from a feed solution to water. Calculations are made for the input parameters shown in Table 1. The concentration distribution of the products of the protonation-deprotonation reactions of ammonia species in the membrane is essentially determined by the local pH value. The shift of the pH in the membrane to the alkaline region leads to the transformation of a part of the NH_4^+ ions into neutral NH_3 molecules. At the left-hand membrane boundary, the concentration of NH_3 exceeds the concentration of NH_4^+ ions by more than two orders of magnitude. At the same time, the concentration profile of these species in the right-hand part of the membrane remains almost constant. But the closer the membrane boundary with dilute solution (initially distilled water), the higher the mole fraction of the molecular form in the couple NH_4^+/NH_3. At the point where the pH value of the internal membrane solution reaches 7.7, the concentrations of NH_4^+ and NH_3 become equal, and at pH ≥ 8.8, the NH_4^+ concentration becomes smaller than the NH_3 concentration. These pH values in the membrane are lower than the corresponding values in solution (see Figure 1), because in the membrane we use the activity coefficients, which are significantly less than 1 for NH_3 and OH^-; all activity coefficients in solution are taken equal to 1.

Preprints (www.preprints.org) | NOT PEER-REVIEWED | Posted: 5 May 2022 doi:10.20944/preprints202205.0055.v1

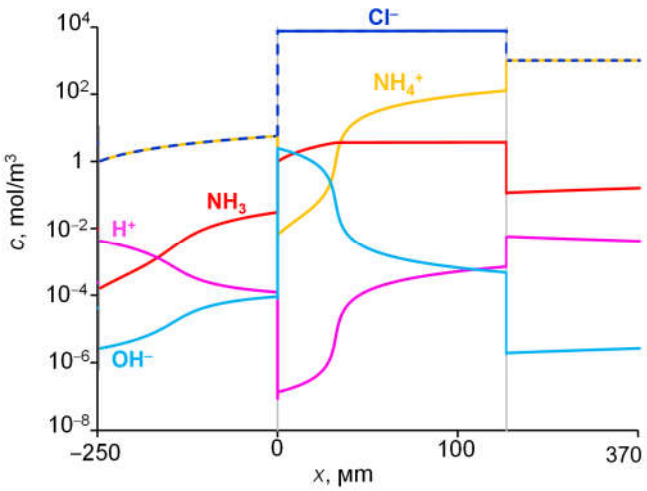

Figure 7. Distribution of ion concentration in the system under study at 1M NH_4Cl solution. Simulation with the input parameters presented in Table 1.

The distribution of fluxes of diffusing species in the membrane system is shown in Figure 8. It can be seen that when approaching the left-hand membrane boundary, a change in the nitrogen atoms carriers occurs, while the magnitude of the flux of these atoms does not change along the coordinate. The nitrogen transfer in the right half of the membrane is carried out mainly by NH_4^+, and in the left half, mainly by NH_3. The NH_3 flux is negligible in the right-hand membrane part, while the NH_4^+ flux is negligible in the left-hand membrane part. When NH_3 exits the membrane into the distillate, these molecules are protonated, and NH_4^+ ions are formed; thus, nitrogen enters the solution as part of the NH_4^+ ions. The released OH^- ions are transferred to the right-hand membrane boundary, these ions are then consumed in the reaction of NH_4^+ deprotonation in the membrane bulk. We assume that NH_3 molecules can move not only through the membrane pores, but through the membrane matrix not containing water; in addition, the effective diffusion coefficient of NH_3 in the membrane is taken greater than that of NH_4^+. For these reasons, the NH_3 flux in the left-hand part of membrane, which is equal to the NH_4^+ flux in the right-hand part (Figure 8), occurs at a lower concentration gradient of NH_3 compared to that of NH_4^+ in the right-hand part of the membrane (Figure 7).

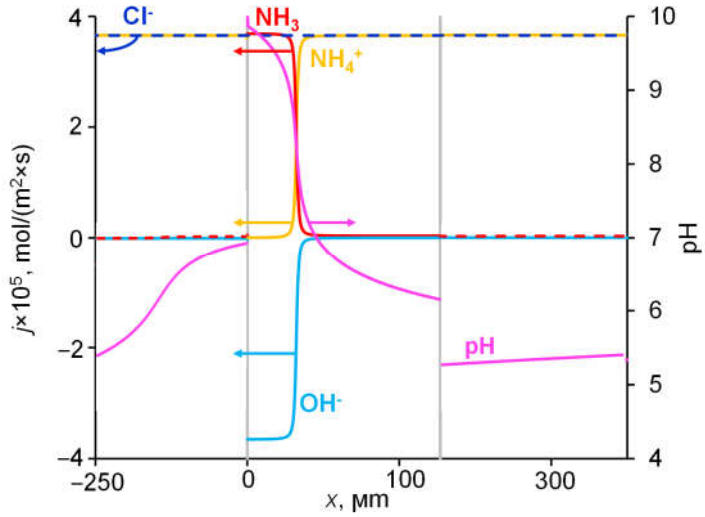

Figure 8. Dependence of the fluxes of all species present in the membrane system and pH dependence on the coordinate. The flux of H^+ ions is negligibly small in all parts of the system and not shown. The secondary y-axis is referred to pH. Simulation for an AMX membrane and 1M NH_4Cl feed solution with the input parameters shown in Table 1.

Preprints (www.preprints.org) | NOT PEER-REVIEWED | Posted: 5 May 2022 doi:10.20944/preprints202205.0055.v1

The rate of NH_3 molecules formation as a function of the coordinate is shown in Figure 9. A small amount of this substance is formed in a narrow reaction zone (~0.03 μm thick) on the right-hand side of the membrane (x=127 μm), where NH_4^+ enters the membrane, in which pH (6.2) is slightly greater than that in the boundary solution (5.3). The main amount of NH_3 is generated in the reaction zone within the membrane bulk, in the vicinity of x=33 μm; the thickness of this zone is ~4 μm. Here, two relatively high fluxes of NH_4^+ and OH^- ions meet moving towards each other. The third reaction region (~0.1 μm thick) is located on the left-hand side of the membrane, where NH_3 molecules disappear to form NH_4^+ and OH^- ions. Here an abrupt shoot of pH occurs when passing from the membrane (pH=10) into solution (pH=6.9). The largest reaction zone is formed in the membrane bulk, where two reactant fluxes gradually decrease in absolute value as they approach the point, at which both fluxes vanish, becoming much less than the flux of NH_3 molecules. When the proton-exchange reactions occur in the interface between two phases, the reaction zone is significantly thinner.

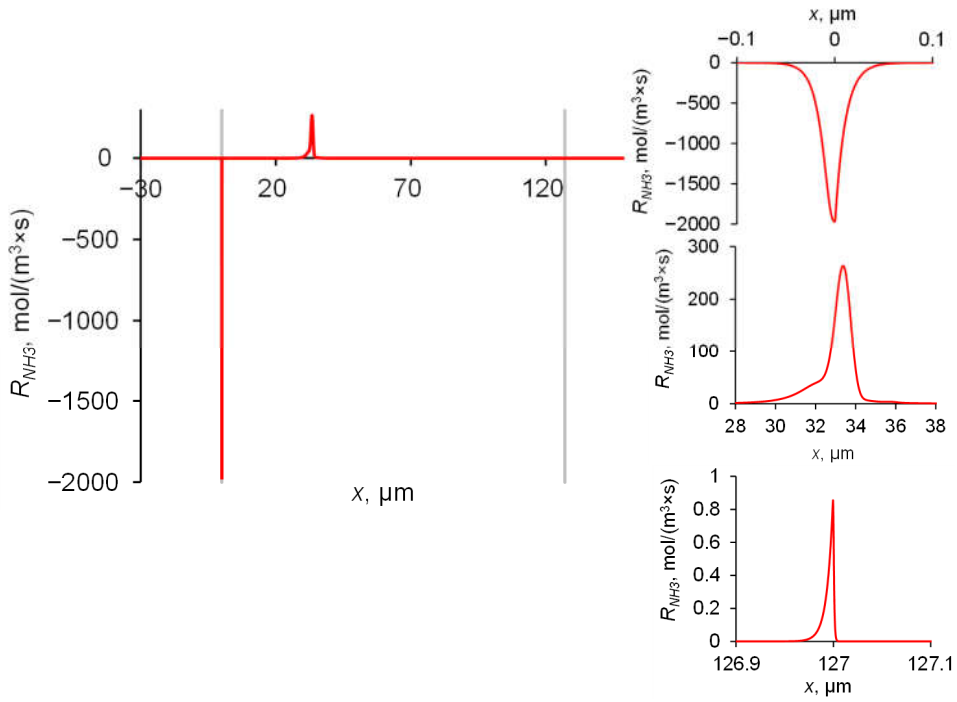

Figure 9. Dependence of the rate of NH_3 molecules' formation on the coordinate. Magnifications of three reaction zones are presented separately in appropriate scales. Simulation for an AMX membrane and 1M NH_4Cl feed solution with the input parameters shown in Table 1.

2.5 Influence of pH of external solution

As it was mentioned above, the concentration of H^+ and OH^- ions in the membrane directly depends on their concentration in the external solution. A change in the pH value of the external solution by 1.5 units leads to a dramatic change in the species concentrations in the membrane (compare Figures 7 and 10). When passing from pH=4 to pH=7 in the feed solution, the concentration of NH_3 at the right-hand side of the membrane increases by almost 3 orders of magnitude (Figures 10a and 10b).

Preprints (www.preprints.org) | NOT PEER-REVIEWED | Posted: 5 May 2022 doi:10.20944/preprints202205.0055.v1

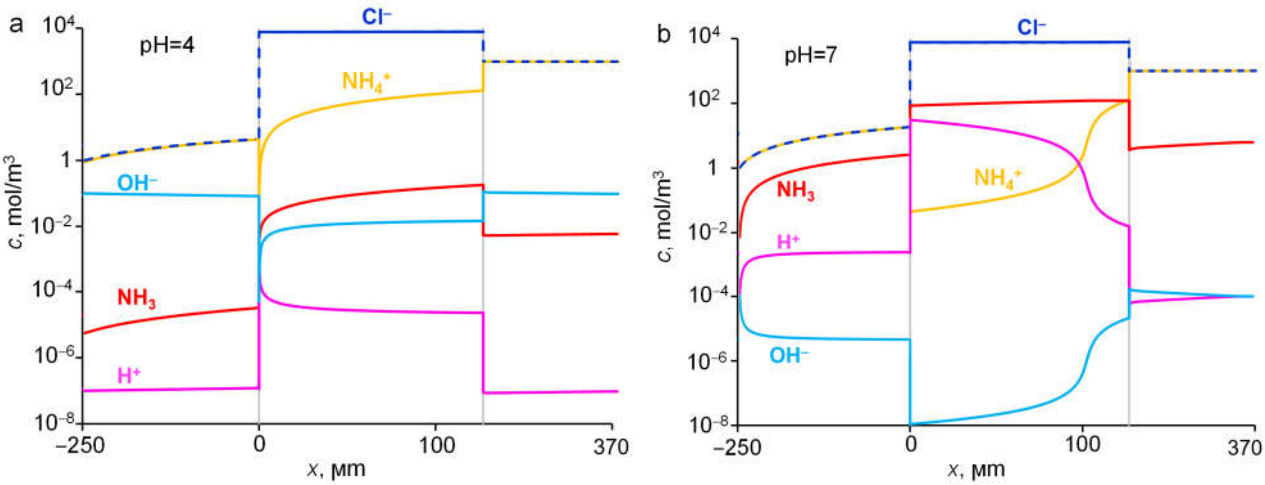

Figure 10. Distribution of species concentrations in the system under study at different pH of the feed 1 M NH_4Cl solution. Simulation, the input parameters are presented in Table 1.

As the pH of the external solution increases, the diffusion flux of NH_4Cl increases (Figure 11). This is of practical importance, since a serious problem in the electrodialysis of ammonium-containing solutions is ammonium back diffusion [54]. Lowering the pH value by adding chemical reagents or creating a reagent-free system using a bipolar membrane would significantly reduce the parasitic ammonium flux. However, in the case of bipolar membranes, reducing the ammonium flux by controlling the pH of the external solution is not possible, since the concentration of H^+ and OH^- ions in such membranes is determined by the rate of water splitting in the bipolar interfacial region [55], and not by the pH of the external solution as in the case of a monopolar membrane.

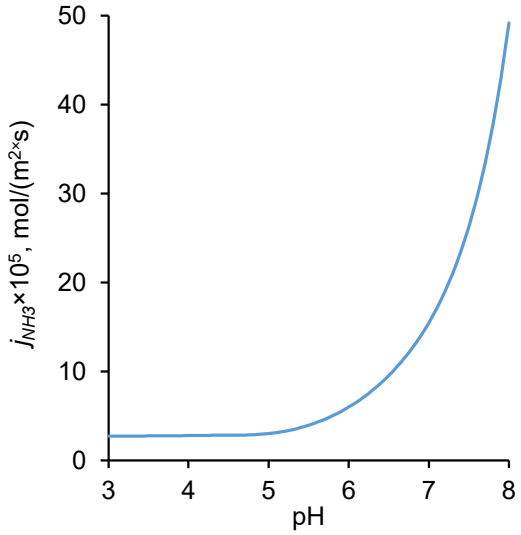

Figure 11. Dependence of the theoretical NH_4Cl flux through an AMX membrane on the pH of the feed electrolyte solution. The input parameters are presented in Table 1.

2.6 Discussion

The results of simulation show that generally, the mechanism of the enhanced permeability of an AEM with respect to NH_4Cl diffusion, schematically depicted in Figure 4, is correct. Indeed, NH_4^+ ions react in the membrane with OH^- ions, thus turning into NH_3

Preprints (www.preprints.org) | NOT PEER-REVIEWED | Posted: 5 May 2022 doi:10.20944/preprints202205.0055.v1

molecules. OH^- ions are generated at the membrane interface facing distilled water when NH_3 molecules leave the membrane and enter the water. However, there is an important detail: the conversion of NH_4^+ into NH_3 occurs not only in the membrane interface facing the feed solution. The degree of conversion increases gradually with increasing distance from the membrane side facing the feed solution and approaching the side facing the dilute solution, that is, as far as the pH of the internal solution rises (Figures 7 and 8). All the membrane volume may be divided in three parts. In the right-hand part, the nitrogen atoms are principally transported by NH_4^+ ions and the flux of NH_3 molecules is negligible; the value of pH changes here from 6.2 to 7.5. In the left-hand part, the nitrogen is mainly transported by NH_3 and the flux of NH_4^+ ions is negligible; pH changes here from 8.8 to 10.0 (Figure 8). There is a narrow central part, where the change of the nitrogen-atom carrier takes place. Within this layer, the fluxes of NH_4^+ and NH_3 are comparable; when passing from the left to the right, the flux of OH^- ions decreases abruptly in absolute value from the value equal to the NH_3 flux at the left side to almost zero at the right side of the membrane. The OH^- ions moving from left to right react with NH_4^+ ions moving in the opposite direction.

Note that the NH_4^+ concentration reaches almost zero at a point close to the middle of the membrane. Therefore, the effective thickness of the diffusion layer for the transport of this ion decreases by about a factor of two compared to the case when the conversion of NH_4^+ ions into NO_3 molecules does not occur. When NO_3 takes over the nitrogen transport, it only needs to pass through the other half of the membrane. Thus, the flux of nitrogen through an anion-exchange membrane during NH_4Cl diffusion can be doubled compared to the transport of another atom (such as potassium), which is carrried by an ion (K^+) with the same mobility as NH_4^+, but cannot be converted into a neutral species during KCl diffusion through the same membrane.

Since the rate constant of this reaction [k_{-1}, Equation (9), Section 4.1] is high, the reaction is limited by the values of the fluxes of OH^- and NH_4^+. OH^- ions are generated at the left side of the membrane, when NH_3 molecules leave the membrane and get into a medium with relatively low pH, where reaction (9) (Section 4.1) occurs. The NH_4^+ ions formed in this reaction transfer from the membrane/solution interface towards the bulk of initially distilled water, and the other product, OH^- ions, move towards the membrane right side. The rate constant of this reaction [k_1, Equation (9)] is also very high. Note that all the rate constants involved in reactions (9)-(11) are high, except for only the water dissociation rate constant, k_d, reaction (11). However, this cannot slow down the resulting rate generation of H^+ and OH^- ions, since they can be obtained in reactions (9) and (10). On the contrary, it can be argued (and this is confirmed in the experiment [19,22]) that the presence of ammonium in a solution subjected to electrodialysis leads to an increase in the rate of H^+/OH^- ion generation near an AEM surface when a sufficiently high current density flows through the membrane. These ions are formed not as a result of water dissociation, reaction (11), but as a result of reactions (9) and (10) of protonation-deprotonation of NH_3 and NH_4^+ particles, respectively. A similar H^+/OH^- ion generation mechanism is described by Simons [56,57] and other authors [58] for substances, presented in solution near an IEM, which can be involved in similar proton-exchange reactions. Since the substances, like NH_3 and NH_4^+ are not used up in this process, and only water molecules are consumed, this process is known as "water splitting". The possibility of this effect occurring in biological membranes is discussed in the literature [57].

It follows from the foregoing that in the system under consideration there are no kinetic limitations on the part of chemical reactions. Therefore, we could reduce the model by assuming local chemical equilibrium not only at the interfaces [Equations (17), (18)], but at any point in the system, and therefore use these equations everywhere instead of Equations (12), (13), (15), (16). However, the use of Equations (12)-(16) only slightly complicates the numerical solution of the mathematical problem. On the other hand, such use makes the model more general and applicable not only at zero electric current, but even at relatively high current densities when some reactions could be kinetically limiting.

Preprints (www.preprints.org) | NOT PEER-REVIEWED | Posted: 5 May 2022 doi:10.20944/preprints202205.0055.v1

The use of the Poisson equation instead of simpler local electroneutrality condition can be characterized similarly to the above: the model with the Poisson equation can be applied not only in the conditions of electrolyte diffusion, but also under electric current flow. There is another advantage of the application of the Poisson equation. When using the local electroneutrality condition, for some input parameters ion concentrations at the interfaces become so small that negative concentrations can appear during the numerical solution process. In this case, the program crashes. When the Poisson equation is applied, this difficulty does not occur.

Note that similar processes can occur in bipolar membranes (BPMs) during their use in electrodialysis of ammonium-containing solution, which explain a very high permeation of ammonia through these membranes known in the literature [25,26,54]. The difference is that the OH^- ions in BPMs are mainly formed in the bipolar interfacial region, where water splitting is enhanced by catalytic participation of fixed functional groups. A high pH value of the internal solution of the anion-exchange layer causes a high concentration of ammonia in this layer, which is the main carrier of the nitrogen atom in it. In the cation-exchange layer, the nitrogen atom is carried by NH_4^+ cations due to a very low pH value in this layer.

Note, that artificial IEM and biological membranes are similar to each other: the design of both provides selectivity with respect to a certain type of ions by the formation of channels/pores that have a specific permeability only for this type of ions. Moreover, the ingenuity of nature, as in many other cases, surpasses that of man: biological membranes have a higher selectivity than synthetic ones. However, with regard to the enhanced transport of ammonium studied here, in the case of biological membranes there is also evidence of undesirable penetration of ammonium ions through a cell membrane that was not intended to be permeable to them [29–31]. The general view of the causes of such elevated NH_4^+ transport through cell membranes is non-ionic diffusion [59,60]. According to this explanation, the ionized form of the compound transforms into its non-ionized configuration upon crossing the membrane surface, which can after that diffuse through the nonpolar region of the cell membrane [60,61]. The model presented in this paper describes such a mechanism in detail from a physicochemical point of view. We believe that this model can be useful not only for specialists in artificial membranes, but also for those who study the selective transport of nitrogen through cell membranes.

3. Experimental part

3.1 Membranes and solutions

Homogeneous ion-exchange membranes Neosepta CMX and AMX (Astom Corp., Japan) manufactured by paste method [62] are used in the study. Both membranes consist of a randomly cross-linked functionated styrenedivinylbenzene copolymer (45-65%) and polyvinylchloride (45-55%) and are reinforced with a polyvinyl chloride mesh. The CMX is a cation-exchange membrane and contains fixed sulfonic groups; the AMX is an anion-exchange membrane and contains quaternary ammonium bases and a small amount of secondary and tertiary amines [63].

The solutions of KCl and NH_4Cl are prepared from a crystalline salt (analytical grade) provided by OJSC Vekton (Russia); the 0.10M KOH solution is prepared from a titrant (manufactured by Uralkhiminvest, Russia). KOH is used to maintain a constant pH value of the solution circulating through the compartments. Distilled water of electrical conductivity 0.8 $\mu S\ cm^{-1}$ and pH=6.2 ± 0.2 at 25°C is used to prepare the solutions.

All membrane samples undergo a standard salt pretreatment [64] and then are equilibrated with 0.02M KCl or 0.02M NH_4Cl solutions before experiments.

3.2 Diffusion permeability

The diffusion characteristics of IEMs were investigated using an experimental setup schematically represented in Figure 12. The two-compartment flow cell is formed by solid plastic frames (1) and a membrane (2), the active surface of which is equal to 7.3 cm^2. The

Preprints (www.preprints.org) | NOT PEER-REVIEWED | Posted: 5 May 2022 doi:10.20944/preprints202205.0055.v1

distance between surfaces of the membrane (2) and the solid plastic frame forming the external wall of the cell is 6.3 mm. The plastic frames with a square aperture are equipped with special comb-shaped guides, which provide the laminar regime of the solution flow in the cell compartments. The membrane separated two streams: distilled water was pumped through one of them (stream I), and a NH_4Cl or KCl solution of a given concentration and pH was pumped through the other stream (II). Before the experiments, all samples were equilibrated with 0.02 M solution of considered electrolyte (NH_4Cl or KCl). The first measurements were carried out for the concentration of electrolyte solution in stream II (Figure 1) equal to 0.02 M. Then, this concentration was sequentially increased to 1.0 M. The membrane under investigation was in contact with each of the solutions for at least 5 hours. The cell scheme, the methodology for conducting the experiment and processing the obtained data are described in detail in [65]. The confidence interval for determining the integral diffusion permeability coefficient of membranes for a given diffusion layer thickness is equal to $\pm 0.4\times10^{-8}$.

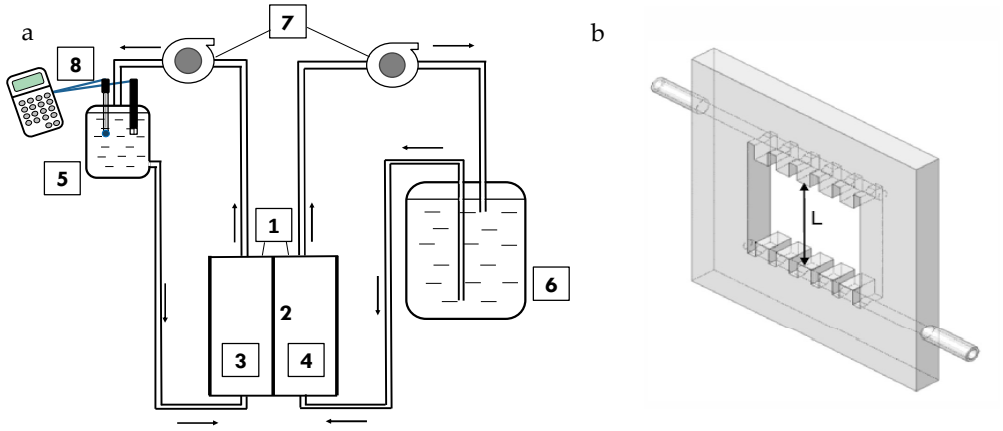

Figure 12. a. Schematic representation of the experimental setup for measuring the membrane diffusion permeability: (1) two-compartment cell, (2) membrane under study confined between two frames shown in b, (3, 4) flow-through compartments of cell (1), (5) container with initially distilled water, (6) container with the electrolyte solution of a given concentration, (7) pumps, (8) conductometric and pH electrodes connected with conductometer and pH meter, respectively; b. plastic frame with special comb-shaped guides of liquid flow.

The integral diffusion coefficient is calculated using the following Equation (4):

$$P = \frac{V_{dw} d}{Sc} \frac{dc_{dw}}{dt} \quad (4)$$

where $\frac{Vdc_{dw}}{Sdt}$ is the flux density of electrolyte diffusion through the membrane, V_{dw} is the volume of the initially distilled water (filling container 5), c_{dw} is the electrolyte concentration in the initially distilled water, S is the membrane area, t is time, c is the concentration of the feed solution (does not change during an experiment).

3.3 Conductivity of IEM

The conductivity of IEM (κ) was determined by a differential method using a clip cell [66,67] and an immittance meter MOTECH MT4080 (Motech Industries Inc., Taiwan) at an alternating current frequency of 1 kHz. All samples were studied in 0.02 M–1.0 M solutions, starting from the lowest concentration.

The conductivity of membranes (κ) is calculated using Equation 5:

$$\kappa = \frac{d}{R_{m+s} - R_s} \quad (5)$$

Preprints (www.preprints.org) | NOT PEER-REVIEWED | Posted: 5 May 2022 doi:10.20944/preprints202205.0055.v1

here R_{m+s} is the resistance of the membrane and solution; R_s is the resistance of the solution.

4. Mathematical Model

4.1. Model formulation

The system under study consists of an anion-exchange membrane of thickness d with two adjacent diffusion layers (DLs): one faces the distilled water on the left side (thickness δ_L) and the other faces the feed solution on the right side (thickness δ_R), as shown in Figure 4. The thickness of both diffusion layers is calculated by the Leveque equation (24). The transport of five species is considered: ammonium ions (NH_4^+), ammonia molecules (NH_3), chloride ions (Cl^-), hydrogen ions (H^+), and hydroxyl ions (OH^-). The transport of the species in the solution and membrane is described by the Nernst-Planck (6), Poisson equation (7) and material balance (8) equation system:

$$j_i = -pD_i\left(\left(1+\frac{d\ln\gamma_i}{d\ln c_i}\right)\frac{\partial c_i}{\partial x}+z_i c_i\frac{F}{RT}\frac{d\varphi}{dx}\right) \quad (6)$$

$$-\varepsilon_r\varepsilon_0\frac{\partial^2\varphi}{\partial x^2}=F\left(\sum_{i=1}^{n}z_i c_i+z_m Q\right) \quad (7)$$

$$\frac{\partial j_i}{\partial x}=pR_i \quad (8)$$

here j_i, D_i, z_i, c_i, γ_i and R_i are the flux density, diffusion coefficient, charge value, concentration, activity coefficient and rate of generation of the i-th species (listed above), respectively; x is the space coordinate; F is the Faraday constant; R is the gas constant; T is the temperature; φ is the electric potential; ε_r is the relative permittivity of the medium; ε_0 is the vacuum permittivity; z_m is the charge value of membrane fixed groups; Q is the concentration of fixed ions; t is time.

It is assumed that the ions mentioned above can transfer through the membrane only inside the pores; therefore, the Nernst-Planck equation in the membrane for these ions is written for the pore solution: the concentrations of mobile and fixed ions are taken in mole/m^3 of the pore solution. To convert the ion flux density found in mole s^{-1}/m^2 of pore cross-section into the unit appropriate for coupling with the flux density in solution, i.e. mole s^{-1}/m^2 of membrane cross-section, we use the coefficient p, which is the membrane porosity p (assumed equal to 0.3 for AMX, as a typical value for membranes made by paste method [68,69]. Evidently, p=1, when considering the transport in solution. As mentioned above, NH_3 molecules can pass not only through pores, but also through uncharged fragments of the membrane matrix. Therefore, to calculate the flow of these species in the membrane, we also take p=1.

To find R_i, three chemical reactions between the species are considered:

$$NH_3 + H_2O \underset{k_{-1}}{\overset{k_1}{\rightleftarrows}} NH_4^+ + OH^- \quad (9)$$

$$NH_4^+ \underset{k_{-2}}{\overset{k_2}{\rightleftarrows}} NH_3 + H^+ \quad (10)$$

$$H_2O \underset{k_r}{\overset{k_d}{\rightleftarrows}} H^+ + OH^- \quad (11)$$

The rates of generation for each species according to Equations (9)-(11) are as follows:

$$R_{NH_3} = -k_1 a_{NH_3} + k_{-1} a_{NH_4^+} a_{OH^-} + k_2 a_{NH_4^+} - k_{-2} a_{NH_3} a_{H^+} \quad (12)$$

$$R_{NH_4^+} = k_1 a_{NH_3} - k_{-1} a_{NH_4^+} a_{OH^-} - k_2 a_{NH_4^+} + k_{-2} a_{NH_3} a_{H^+} \quad (13)$$

Preprints (www.preprints.org) | NOT PEER-REVIEWED | Posted: 5 May 2022 doi:10.20944/preprints202205.0055.v1

$$R_{Cl^-} = 0 \tag{14}$$

$$R_{H^+} = k_2 a_{NH_4^+} - k_{-2} a_{NH_3} a_{H^+} + k_d a_{H_2O} - k_r a_{H^+} a_{OH^-} \tag{15}$$

$$R_{OH^-} = k_1 a_{NH_3} - k_{-1} a_{NH_4^+} a_{OH^-} + k_d a_{H_2O} - k_r a_{H^+} a_{OH^-} \tag{16}$$

where a_i is the activity of i-th species, k_i are the rate constants of protonation-deprotonation reactions presented in Equations (9)-(11).

4.2 Boundary conditions

Equations (6)-(8) are valid for both DLs and membrane. However, the values of the diffusion coefficients, activity coefficients, porosity, concentration of the fixed ions, and relative permittivity in DLs and membrane are different. These parameters smoothly vary at the membrane/solution interface (i.e. at x=0 and x=d) from the values in the solution to those in the membrane. The thickness of interface transition regions is chosen to be 1 nm, which is close to the value of dense part of double electrical layer [70]. To describe these changes, the rectangle function (in Comsol software) is used. It was verified that a small variation in the transition region thickness (in the range from 1 to 2 nm) and the shape of the function describing the variation of the parameters does not affect the results of the numerical solution.

It is assumed that at x=0 and x=d there is a local equilibrium of reactions (9)-(11), which is described by the following equations:

$$K_b = \frac{k_1}{k_{-1}} = \frac{a_{NH_4^+} a_{OH^-}}{a_{NH_3}}, \quad K_a = \frac{k_2}{k_{-2}} = \frac{a_{NH_3} a_{H^+}}{a_{NH_4^+}} \tag{17}$$

$$K_w = \frac{k_d}{k_r} = a_{H^+} a_{OH^-} \tag{18}$$

where K_b is the base ionization constant of ammonia; K_w is the water dissociation constant; k_1 and k_{-1} are the rate constants of forward and revers reaction (9), respectively; k_2 and k_2 are the rate constants of forward and revers reaction (10), respectively; k_d is the rate constant of water dissociation; k_r is the rate constant of recombination H^+ and OH^-.

The concentrations of all species at x=$-\delta_L$ are zero, except of concentrations of H^+ and OH^- since there is distilled water in the bulk of the left-hand solution with pH=5.4; at x=d+δ_R the concentrations, c_i^{0R}, are known from the experimental conditions:

$$c_i(x = -\delta_L) = 0, \text{ i=NH}_3, \text{ NH}_4^+, \text{ K}^+, \text{ Cl}^-; \; c_{H^+}(x = -\delta_L) = 10^{-5.4}; \; c_{OH^-}(x = -\delta_L) = 10^{-8.6} \tag{19}$$

$$c_i(x = d + \delta_R) = c_i^{0R} \tag{20}$$

The concentration of chloride ions and pH value in the feed solution are set for each experimental run. Then the concentrations of hydrogen and hydroxyl ions can be calculated from the known pH. The concentration of ammonium ions can be calculated using the electroneutrality assumption: $c_{NH_4^+} = c_{Cl^-} + c_{OH^-} - c_{H^+}$.

The concentration of ammonia is calculated from Equation (17), the activity coefficients are set equal to 1:

$$c_{NH_3}^0 = \frac{K_a \cdot c_{NH_4^+}^0}{c_{H^+}^0} \tag{21}$$

At the x=$-\delta_L$ the electrical potential equals zero:

$$\varphi(x = -\delta_L) = 0 \tag{22}$$

At the x=$-\delta_R$ and x=$-\delta_L$ the current density, j, equals zero:

Preprints (www.preprints.org) | NOT PEER-REVIEWED | Posted: 5 May 2022 doi:10.20944/preprints202205.0055.v1

$$j = F\sum_i J_i z_i = 0 \tag{23}$$

4.3 Determination of input parameters

The diffusion boundary layer thickness in the experimental cell is calculated using the Leveque equation [71]

$$\delta = 1.02\left(\frac{LDh}{\overline{V}}\right)^{1/3} \tag{24}$$

here L is the channel length, D is the electrolyte diffusion coefficient, h is the distance between the studied membrane and the cell wall, $\overline{V}$ is the linear flow velocity.

Reaction rate constants. According to Simons [56], the rate constants k_{-1} and k_{-2} of recombination reactions (9) and (10) in free solution have high values of the order of 10^{10} $dm^3\ mol^{-1}\ s^{-1}$. The rate constants k_1 and k_2 of direct reactions (9) and (10) (considered as pseudomonomolecular) can be estimated using the following relations [23]:

$$k_1 = k_{-1}10^{-(14-pK_a)},\ k_2 = k_{-2}10^{-pK_a} \tag{25}$$

The calculation using equation (25) gives $k_1 \approx 10^6\ s^{-1}$, $k_2 \approx 10\ s^{-1}$. Thus, the rate limiting stage of protonation-deprotonation reactions (9) and (10) is the NH_4^+ deprotonation reaction. However, the value of the rate constant of this reaction (k_2) is quite high. It is almost 6 orders of magnitude higher than the rate constant of water dissociation in free solution (2×10^{-5} s^1) , 4 orders of magnitude higher than in the case of sulfonic groups, 3×10^{-3} s^{-1} [72] (the CMX membrane) and 2 orders of magnitude higher than in the case of secondary and tertiary amino groups, 10^{-1} s^{-1} [72] (the AMX membrane). Thus, NH_4^+/NH_3 couple may be considered as a catalyst for the reaction of H^+ and OH^- ions generation. The latter is important for electrodialysis of ammonium-containing solutions, where water splitting reactions are of great impact.

Diffusion coefficients. The model assumes that the membrane is a quasi-homogeneous medium. The diffusion coefficients may be estimated from the equation system, describing the conductivity, κ , and differential diffusion permeability, $\overline{P}$, of the membrane [48]:

$$\overline{P} = \overline{t_1}\left(1-\frac{z_2}{z_1}\right)\frac{\overline{D}_2\overline{c}_2}{c_2} \tag{26}$$

$$\kappa = \frac{F^2}{RT}\left(z_1^2\overline{D}_1\overline{c}_1 + z_2^2\overline{D}_2\overline{c}_2\right) \tag{27}$$

$$\overline{t_i} = \frac{z_i^2\overline{D}_i\overline{c}_i}{z_1^2\overline{D}_1\overline{c}_1 + z_2^2\overline{D}_2\overline{c}_2} \tag{28}$$

where subscript 1 and 2 refer to the counterion and coion, respectively, $\overline{t_i}$ is the transport number of ion i in the membrane.

Since $\overline{t_1}$ is close to 1, it can be seen from Equation (26) that $\overline{P}$ is mainly determined by the product $\overline{D}_2\overline{c}_2$ at a given concentration of the external solution, c_2. As $\overline{D}_2\overline{c}_2 << \overline{D}_1\overline{c}_1$, the membrane conductivity is controlled by the product $\overline{D}_1\overline{c}_1$, Equation (27). At a given concentration of the external solution and known values of κ and $\overline{P}$, it is possible to calculate $\overline{D}_1$ and $\overline{D}_2$:

$$\overline{D}_2 = \frac{c_2\overline{P}}{\overline{t_1}\overline{c}_2\left(1-z_2/z_1\right)} \tag{29}$$

$$\overline{D}_1 = \frac{\kappa RT/F^2 - z_2^2\overline{D}_2\overline{c}_2}{z_1 Q - z_1 z_2\overline{c}_2} \tag{30}$$

Preprints (www.preprints.org) | NOT PEER-REVIEWED | Posted: 5 May 2022 doi:10.20944/preprints202205.0055.v1

the Donnan constant, K_D, is needed to relate the coion concentrations in the solution and membrane; in its approximate form, the Donnan equation reads [44,48]: $\bar{c}_2 = \frac{K_D}{Q} c_2^2$; $\bar{c}_1$ can be found using the local electroneutrality condition ($z_1\bar{c}_1 + z_2\bar{c}_2 = Q$).

Note that $\bar{P}$ is the differential diffusion permeability, while the experiment gives the integral diffusion permeability, P. It is possible to convert the concentration dependence of $P(c)$ into $\bar{P}(c)$ [48]:

$$\bar{P}(c) = P(c) + d\lg P / d\lg c \quad (30)$$

and then calculate $\bar{D}_1$ and $\bar{D}_2$.

In the case of AMX/KCl, this way of determination of $\bar{D}_1$ and $\bar{D}_2$ gives correct values, which are present in Table 1; the comparison of experimental and simulated concentration dependencies of κ and P is shown in Figure 5. Since the value of κ is very close for the AMX in KCl and NH_4Cl solutions, the Cl^- diffusion coefficient, $\bar{D}_1$, in the membrane was taken the same for both cases, $\bar{D}_{Cl^-}$ =2.7×10⁻¹¹ m²/s (Table 1). Since in the solution the diffusion coefficients of NH_4^+ and Cl^- are nearly identical, we assume the egality of these coefficients in the membrane: $\bar{D}_{K^+} = \bar{D}_{NH_4^+}$ =2.7×10⁻¹¹ m²/s (Table 1).

The concentration of fixed groups in the pore solution of the AMX membrane is calculated from the value of the exchange capacity of this membrane в Cl^- form by dividing the latter by the membrane porosity p=0.3; the obtained value is Q= 7.6 mol/dm³ H_2O [68], Table 1. The value of ε is taken as 80 in solution [28] and 30 in the membrane [73].

Table 1. Input parameters of the model for the system under study

Parameter	Description	Value	Reference
d	membrane thickness	AMX 127 μm	*
		CMX 172 μm	*
δ_L=δ_R	diffusion layer thickness	247 μm	Eq. (24)
	KCl (NH_4Cl) electrolyte diffusion coefficient in solution	1.99×10⁻⁹ m²/s	
K_a	acid dissociation constant of NH_3	5.62×10⁻⁷ mol/m³	[28]
K_w	water dissociation constant	10⁻⁸ mol²/m⁶	[28]
k_1	rate constant of forward reaction (3)	1.78×10⁵ s⁻¹	Eq. (25)
k_{-1}	rate constant of backward reaction (3)	10⁷ m³/(s×mol)	k_1×K_b
k_2	rate constant of forward reaction (4)	5.63 s⁻¹	Eq. (25)
k_{-2}	rate constant of backward reaction (4)	10⁷ m³/(s×mol)	k_2×K_a
k_d	rate constant of water dissociation	2×10⁻⁵ s⁻¹	[56]
k_r	rate constant of water recombination	1.18×10⁸ m³/(s×mol)	k_d/(K_w×c_w)
c_w	concentration of water	5.55×10⁴ mol/m³	
D_{NH_3}	diffusion coefficients of species in solutions	1.64×10⁻⁹ m²/s	[74]
$D_{NH_4^+}$		1.96×10⁻⁹ m²/s	[28]
D_{Cl^-}		2.03×10⁻⁹ m²/s	[28]
D_{H^+}		9.3×10⁻⁹ m²/s	[28]
D_{OH^-}		5.3×10⁻⁹ m²/s	[28]
D_{K^+}		1.96×10⁻⁹ m²/s	[28]
$\bar{D}_{NH_3}$	diffusion coefficient of species in the membrane	4.4×10⁻¹⁰ m²/s	
$\bar{D}_{NH_4^+}$		2.7×10⁻¹¹ m²/s	*
$\bar{D}_{Cl^-}$		2.7×10⁻¹¹ m²/s	*
$\bar{D}_{H^+}$		2.8×10⁻⁹ m²/s	

 doi:10.20944/preprints202205.0055.v1

$\bar{D}_{OH^-}$		1.6×10^{-9} m²/s	
$\bar{D}_{K^+}$		2.7×10^{-11} m²/s	*
γ_{NH_3}	activity coefficients of species in membrane	0.03	**
$\gamma_{NH_4^+}$		1	
γ_{Cl^-}		1	
γ_{H^+}		1	**
γ_{OH^-}		0.03	**
γ_{K^+}		1	
ε_s	relative permittivity in solution	80	[28]
ε_m	relative permittivity in membrane	30	[73]
Q	ion-exchange capacity	7600 mol/m³ H_2O	[68]
pH	pH value in both streams	5.4	*
$c_{Cl^-}^{0R}$	chloride ions concentration at x=d+δ_R	0.1-1 M	*
p	porosity	0.3	

* – parameters are from an independent experiment
** – fitting parameters

The mathematical problem was solved numerically by finite element method using the Comsol Multiphysics 5.6 commercial software package.

4. Conclusions

We proposed a new one-dimensional model to explain an enhanced diffusion of ammonium chloride through anion-exchange membranes. Diffusion and migration transport of ions as well as proton-exchange reactions between NH_4Cl, NH_3 and water are taken into account. It is assumed that NH_4^+, Cl^- and OH^- ions can only pass through the hydrophilic pores of an AEM, while NH_3 can diffuse both through the pores and through fragments of the membrane matrix that do not contain water. Another reason for a high NH_4Cl diffusion is a lower value of the effective diffusion layer, δ_{ef}, which controls the rate of diffusion. In the case of KCl diffusion through the same membrane, δ_{ef} is equal to the membrane thickness, while in the case of NH_4Cl diffusion, it is approximately two time lower. The latter is caused by the fact that the concentration of NH_4^+ reach almost zero value close to the middle of the membrane. In the other half-part of the membrane, the nitrogen-atom is carried by NH_3 molecules. These molecules are formed in the membrane due to the reaction between NH_4^+ and OH^- ions. The latter are generated at the membrane interface facing distilled water when NH_3 molecules leave the membrane and enter the water.

The model overall correctly describes the concentration dependence of the diffusion permeability and electrical conductivity of an anion-exchange membrane (a Neosepta AMX membrane) in NH_4Cl and KCl solutions. However, the experimental dependence is steeper than the calculated one. The reason is that the model does not take into account the contribution of ion transfer in an electrically neutral solution that fills the macropores and central parts of the mesopores of the membrane. This contribution can be taken into account when combining the proposed model and the known micro-heterogeneous model. However, at this stage of our study this combination seems to be difficult to realize. We plan to make it in the future.

The model gives also an insight into understanding of high permeability of ammonia through bipolar membranes during electrodialysis of ammonium-containing solution. The difference is that the OH^- ions are mainly formed at the bipolar interfacial region, where water splitting enhanced by catalytic participation of fixed functional groups takes place. A high pH value of the internal solution of the anion-exchange layer causes a high concentration of ammonia in this layer, which is the main carrier of the nitrogen atom. In

 doi:10.20944/preprints202205.0055.v1

the cation-exchange layer, nitrogen-atom is carried by NH_4^+ cations due to a very low pH value in this layer.

We also believe that the model can be useful for a better understanding of nitrogen transport across biological cell membranes.

Author Contributions: Conceptualization, E.S., N.P., V.N. and S.M.; methodology, N.P. and S.M.; software, E.S. and S.M.; validation, E.S., E.M. and S.M.; formal analysis, S.M. and E.M.; investigation, K.T., E.S., S.M. and N.P.; resources, N.P.; writing—original draft preparation, S.M. and E.S.; writing—review and editing, V.N. and N.P.; visualization, E.S., K.T and S.M.; supervision, V.N.; project administration, N.P.; funding acquisition, N.P. All authors have read and agreed to the published version of the manuscript.

Funding: This research was funded by the Kuban Science Foundation, MFI-20.1/128.

Institutional Review Board Statement: Not applicable.

Informed Consent Statement: Not applicable.

Data Availability Statement: Not applicable.

Conflicts of Interest: The authors declare no conflict of interest.

References

[1] USEPA, Preventing Eutrophication: Scientific Support for Dual Nutrient Criteria, 2015.

[2] A.R. Ravishankara, J.S. Daniel, R.W. Portmann, Nitrous oxide (N2O): The dominant ozone-depleting substance emitted in the 21st century, Science (80-.). 326 (2009) 123–125. https://doi.org/10.1126/science.1176985.

[3] D.E. Canfield, A.N. Glazer, P.G. Falkowski, The evolution and future of earth's nitrogen cycle, Science (80-.). 330 (2010) 192–196. https://doi.org/10.1126/science.1186120.

[4] D.M. Anderson, J.M. Burkholder, W.P. Cochlan, P.M. Glibert, C.J. Gobler, C.A. Heil, R.M. Kudela, M.L. Parsons, J.E.J. Rensel, D.W. Townsend, V.L. Trainer, G.A. Vargo, Harmful algal blooms and eutrophication: Examining linkages from selected coastal regions of the United States, Harmful Algae. 8 (2008) 39–53. https://doi.org/10.1016/j.hal.2008.08.017.

[5] V. Smil, Nitrogen and food production: Proteins for human diets, Ambio. 31 (2002) 126–131. https://doi.org/10.1579/0044-7447-31.2.126.

[6] H.C.J. Godfray, J.R. Beddington, I.R. Crute, L. Haddad, D. Lawrence, J.F. Muir, J. Pretty, S. Robinson, S.M. Thomas, C. Toulmin, Food Security: The Challenge of Feeding 9 Billion People, Science (80-.). 327 (2017) 812–818. https://doi.org/10.1109/CIS.2016.52.

[7] S. Giddey, S.P.S. Badwal, A. Kulkarni, Review of electrochemical ammonia production technologies and materials, Int. J. Hydrogen Energy. 38 (2013) 14576–14594. https://doi.org/10.1016/j.ijhydene.2013.09.054.

[8] C. Philibert, Renewable energy for industry, in: IJISEA Annu. Meet. NREL, Golden, 2018. http://admin.indiaenvironmentportal.org.in/files/file/Renewable Energy for Industry.pdf.

[9] Y. V. Nancharaiah, S. Venkata Mohan, P.N.L. Lens, Recent advances in nutrient removal and recovery in biological and bioelectrochemical systems, Bioresour. Technol. 215 (2016) 173–185. https://doi.org/10.1016/j.biortech.2016.03.129.

[10] R. Lan, S. Tao, Direct ammonia alkaline anion-exchange membrane fuel cells, Electrochem. Solid-State Lett. 13 (2010) 8–11. https://doi.org/10.1149/1.3428469.

[11] Y. Katayama, T. Okanishi, H. Muroyama, T. Matsui, K. Eguchi, Enhancement of ammonia oxidation activity over Y2O3-modified platinum surface: Promotion of NH2,ad dimerization process, J. Catal. 344 (2016) 496–506. https://doi.org/10.1016/j.jcat.2016.10.020.

[12] Y. Aoki, T. Yamaguchi, S. Kobayashi, D. Kowalski, C. Zhu, H. Habazaki, High-Efficiency Direct Ammonia Fuel Cells Based on BaZr 0.1 Ce 0.7 Y 0.2 O 3− δ /Pd Oxide-Metal Junctions , Glob. Challenges. 2 (2018) 1700088. https://doi.org/10.1002/gch2.201700088.

[13] T. Lipman, N. Shah, Ammonia as an Alternative Energy Storage Medium for Hydrogen Fuel Cells, Escholarsh. Repos. Univ.

Calif. (2007). https://escholarship.org/uc/item/7z69v4wp.

[14] C.M. Mehta, W.O. Khunjar, V. Nguyen, S. Tait, D.J. Batstone, Technologies to recover nutrients from waste streams: A critical review, Crit. Rev. Environ. Sci. Technol. 45 (2015) 385–427. https://doi.org/10.1080/10643389.2013.866621.

[15] M. Rodríguez Arredondo, P. Kuntke, A.W. Jeremiasse, T.H.J.A. Sleutels, C.J.N. Buisman, A. Ter Heijne, Bioelectrochemical systems for nitrogen removal and recovery from wastewater, Environ. Sci. Water Res. Technol. 1 (2015) 22–33. https://doi.org/10.1039/c4ew00066h.

[16] A.J. Ward, K. Arola, E. Thompson Brewster, C.M. Mehta, D.J. Batstone, Nutrient recovery from wastewater through pilot scale electrodialysis, Water Res. 135 (2018) 57–65. https://doi.org/10.1016/j.watres.2018.02.021.

[17] S. Melnikov, S. Loza, M. Sharafan, V. Zabolotskiy, Electrodialysis treatment of secondary steam condensate obtained during production of ammonium nitrate. Technical and economic analysis, Sep. Purif. Technol. 157 (2016) 179–191. https://doi.org/10.1016/j.seppur.2015.11.025.

[18] X. Wang, X. Zhang, Y. Wang, Y. Du, H. Feng, T. Xu, Simultaneous recovery of ammonium and phosphorus via the integration of electrodialysis with struvite reactor, J. Memb. Sci. 490 (2015) 65–71. https://doi.org/10.1016/j.memsci.2015.04.034.

[19] O.A. Kozaderova, S.I. Niftaliev, K.B. Kim, Ionic Transport in Electrodialysis of Ammonium Nitrate, Russ. J. Electrochem. 54 (2018) 363–367. https://doi.org/10.1134/S1023193518040043.

[20] O.A. Kozaderova, K.B. Kim, C.S. Gadzhiyeva, S.I. Niftaliev, Electrochemical characteristics of thin heterogeneous ion exchange membranes, J. Memb. Sci. 604 (2020). https://doi.org/10.1016/j.memsci.2020.118081.

[21] O.M. Aminov, V.A. Shaposhnik, A.A. Guba, A.E. Kutsenko, Coupled transport of ammonium ions with hydrogen and hydroxide ions during electrodialysis in the region of overlimiting current densities, Sorption Chromatogr. Process. 13 (2013) 816–822.

[22] O.A. Rybalkina, K.A. Tsygurina, E.D. Melnikova, G. Pourcelly, V.V. Nikonenko, N.D. Pismenskaya, Catalytic effect of ammonia-containing species on water splitting during electrodialysis with ion-exchange membranes, Electrochim. Acta. 299 (2019) 946–962. https://doi.org/10.1016/j.electacta.2019.01.068.

[23] H. Yan, L. Wu, Y. Wang, M. Irfan, C. Jiang, T. Xu, Ammonia capture from wastewater with a high ammonia nitrogen concentration by water splitting and hollow fiber extraction, Chem. Eng. Sci. 227 (2020) 115934. https://doi.org/10.1016/j.ces.2020.115934.

[24] L. Franck-Lacaze, P. Sistat, P. Huguet, Determination of the pKa of poly (4-vinylpyridine)-based weak anion exchange membranes for the investigation of the side proton leakage, J. Memb. Sci. 326 (2009) 650–658. https://doi.org/10.1016/j.memsci.2008.10.054.

[25] L. Shi, L. Xiao, Z. Hu, X. Zhan, Nutrient recovery from animal manure using bipolar membrane electrodialysis: Study on product purity and energy efficiency, Water Cycle. 1 (2020) 54–62. https://doi.org/10.1016/j.watcyc.2020.06.002.

[26] D. Saabas, J. Lee, Recovery of ammonia from simulated membrane contactor effluent using bipolar membrane electrodialysis, J. Memb. Sci. 644 (2022) 120081. https://doi.org/10.1016/j.memsci.2021.120081.

[27] N. van Linden, G.L. Bandinu, D.A. Vermaas, H. Spanjers, J.B. van Lier, Bipolar membrane electrodialysis for energetically competitive ammonium removal and dissolved ammonia production, J. Clean. Prod. 259 (2020) 120788. https://doi.org/10.1016/j.jclepro.2020.120788.

[28] D.R. Lide, G. Baysinger, L.I. Berger, H. V Kehiaian, D.L. Roth, D. Zwillinger, R.N. Goldberg, W.M. Haynes, CRC Handbook of Chemistry and Physics, CRC Press, New York, 1997.

[29] S.M. Howitt, M.K. Udvardi, Structure, function and regulation of ammonium transporters in plants, Biochim. Biophys. Acta - Biomembr. 1465 (2000) 152–170. https://doi.org/10.1016/S0005-2736(00)00136-X.

[30] A.S. Verkman, A.K. Mitra, Structure and function of aquaporin water channels, Am. J. Physiol. - Ren. Physiol. 278 (2000) F12–F28. https://doi.org/10.1016/j.envpol.2004.10.021.

[31] P. Agre, The aquaporin water channels., Proc. Am. Thorac. Soc. 3 (2006) 5–13. https://doi.org/10.1513/pats.200510-109JH.

[32] M. Meuwly, A. Bach, S. Leutwyler, Grotthus-type and diffusive proton transfer in 7-hydroxyquinoline·(NH3)n clusters, J. Am. Chem. Soc. 123 (2001) 11446–11453. https://doi.org/10.1021/ja010893a.

[33] D.W. Lim, M. Sadakiyo, H. Kitagawa, Proton transfer in hydrogen-bonded degenerate systems of water and ammonia in metal-organic frameworks, Chem. Sci. 10 (2019) 16–33. https://doi.org/10.1039/C8SC04475A.

[34] E.D. Melnikova, K.A. Tsygurina, N.D. Pismenskaya, V. V. Nikonenko, Influence of Protonation-Deprotonation Reactions on Diffusion of Ammonium Chloride through an Anion Exchange Membrane, Membr. Membr. Technol. 11 (2021) 360–370. https://doi.org/10.1134/s2218117221050084.

[35] V.I. Vasil'eva, V.A. Shaposhnik, I.A. Zemlyanukhina, O. V. Grigorchuk, Facilitated diffusion of amino acids in ion-exchange membranes, Russ. J. Phys. Chem. A. 77 (2003) 1017–1019.

[36] V. Vasil'eva, E. Goleva, N. Pismenskaya, A. Kozmai, V. Nikonenko, Effect of surface profiling of a cation-exchange membrane on the phenylalanine and NaCl separation performances in diffusion dialysis, Sep. Purif. Technol. 210 (2019) 48–59. https://doi.org/10.1016/j.seppur.2018.07.065.

[37] K. Ueno, T. Doi, B. Nanzai, M. Igawa, Selective transport of neutral amino acids across a double-membrane system comprising cation and anion exchange membranes, J. Memb. Sci. 537 (2017) 344–352. https://doi.org/10.1016/j.memsci.2017.04.013.

[38] R.J. Ouellette, J.D. Rawn, 31 - Lipids and Biological Membranes, in: R.J. Ouellette, J.D. Rawn (Eds.), Org. Chem. (Second Ed., Second Edi, Academic Press, 2018: pp. 1001–1032. https://doi.org/https://doi.org/10.1016/B978-0-12-812838-1.50031-1.

[39] Y. Liu, M. Qin, S. Luo, Z. He, R. Qiao, Understanding Ammonium Transport in Bioelectrochemical Systems towards its Recovery, Sci. Rep. 6 (2016) 1–10. https://doi.org/10.1038/srep22547.

[40] F.G. Helfferich, Ion Exchange, McGraw-Hill, 1962.

[41] Y. Ji, H. Luo, G.M. Geise, Specific co-ion sorption and diffusion properties influence membrane permselectivity, J. Memb. Sci. 563 (2018) 492–504. https://doi.org/10.1016/j.memsci.2018.06.010.

[42] A.N. Filippov, N.A. Kononenko, O.A. Demina, Diffusion of electrolytes of different natures through the cation-exchange membrane, Colloid J. 79 (2017) 556–566. https://doi.org/10.1134/S1061933X17040044.

[43] O.A. Demina, N.A. Kononenko, И.V. Falina, A.V. Demin, Theoretical Estimation of Differential Diffusion Permeability Coefficients of Ion Exchange Membranes, Colloid J. 79 (2017) 259–269. https://doi.org/10.7868/s0023291217030041.

[44] V. V. Nikonenko, A.B. Yaroslavtsev, G. Pourcelly, Ion Transfer in and Through Charged Membranes: Structure, Properties, and Theory, in: Ion. Interact. Nat. Synth. Macromol., John Wiley & Sons, Inc., Hoboken, NJ, USA, 2012: pp. 267–335. https://doi.org/10.1002/9781118165850.ch9.

[45] R. Mills, V.M.M. Lobo, Self-diffusion in electrolyte solutions. A critical examination of data compiled from the literature, Elsevier Science Publishers B.V., 1989.

[46] W. Hua, D. Verreault, Z. Huang, E.M. Adams, H.C. (Ohio S.U. Allen, Z. Huang, H.C. (Ohio S.U. Allen, E.M. Adams, Z. Huang, Cation Effects on Interfacial Water Organization of Aqueous Chloride Solutions. I. Monovalent Cations: Li+, Na+, K+, and NH4+, J. Phys. Chem. B. 118 (2014) 8433–8440. file:///Users/nishasheth/Box Sync/Literature and References/Articles/Water Absorption/Hydrogen Bonds/Cation Effects on Interfacial Water Organization of Aqueous Chloride Solutions. I. Monovalent Cations- Li+, Na+, K+, and NH4 +.pdf.

[47] A. Fuocco, H. Zwijnenberg, S. Galier, H. Roux-de Balman, G. De Luca, Structural properties of cation exchange membranes: Characterization, electrolyte effect and solute transfer, J. Memb. Sci. 520 (2016) 45–53.

[48] V.I. Zabolotsky, V.V. Nikonenko, Effect of structural membrane inhomogeneity on transport properties, J. Memb. Sci. 79 (1993) 181–198. https://doi.org/10.1016/0376-7388(93)85115-D.

[49] A. Bhown, E.L. Cussler, Mechanism for Selective Ammonia Transport through Poly(vinylammonium thiocyanate) Membranes, J. Am. Chem. Soc. 113 (1991) 742–749. https://doi.org/10.1021/ja00003a002.

[50] W.A. Phillip, E. Martono, L. Chen, M.A. Hillmyer, E.L. Cussler, Seeking an ammonia selective membrane based on

nanostructured sulfonated block copolymers, J. Memb. Sci. 337 (2009) 39–46. https://doi.org/10.1016/j.memsci.2009.03.013.

[51] G.P. Pez, D. V. Laciak, United States Patent №4762535 "Ammonia separation using semipermeable membranes," 1988.

[52] N.P. Berezina, N.A. Kononenko, O.A. Dyomina, N.P. Gnusin, Characterization of ion-exchange membrane materials: Properties vs structure, Adv. Colloid Interface Sci. 139 (2008) 3–28. https://doi.org/10.1016/j.cis.2008.01.002.

[53] J. Kamcev, D.R. Paul, B.D. Freeman, Effect of fixed charge group concentration on equilibrium ion sorption in ion exchange membranes, J. Mater. Chem. A. 5 (2017) 4638–4650. https://doi.org/10.1039/c6ta07954g.

[54] N. van Linden, H. Spanjers, J.B. van Lier, Application of dynamic current density for increased concentration factors and reduced energy consumption for concentrating ammonium by electrodialysis, Water Res. 163 (2019) 114856. https://doi.org/10.1016/j.watres.2019.114856.

[55] V.I. Zabolotskii, N. V Shel'deshov, N.P. Gnusin, Dissociation of Water Molecules in Systems with Ion-exchange Membranes, Russ. Chem. Rev. 57 (1988) 801–808. https://doi.org/10.1070/rc1988v057n08abeh003389.

[56] R. Simons, Electric field effects on proton transfer between ionizable groups and water in ion exchange membranes, Electrochim. Acta. 29 (1984) 151–158. https://doi.org/10.1016/0013-4686(84)87040-1.

[57] R. Simons, Water splitting in ion exchange membranes, Electrochim. Acta. 30 (1985) 275–282. https://doi.org/10.1016/0013-4686(85)80184-5.

[58] Y. Tanaka, Acceleration of water dissociation generated in an ion exchange membrane, J. Memb. Sci. 303 (2007) 234–243. https://doi.org/10.1016/J.MEMSCI.2007.07.020.

[59] B.W. Brazier, Membrane Transport of Nutrients, Am. J. Food Nutr. 4 (2001) 135–137. https://doi.org/10.1016/b978-012655330-7/50063-0.

[60] K. Barrett, H. Brooks, S. Boitano, S. Barman, Ganong's Review of Medical Physiology, 2010.

[61] S. Silbernagl, D. Scheller, Formation and Excretion of NH3- NH4+. New Aspects of an old problem, Klinsche Wochenschrift. 64 (1986) 862–870.

[62] Y. Mizutani, Structure of ion exchange membranes, J. Memb. Sci. 49 (1990) 121–144. https://doi.org/10.1016/S0376-7388(00)80784-X.

[63] E. Güler, W. van Baak, M. Saakes, K. Nijmeijer, Monovalent-ion-selective membranes for reverse electrodialysis, J. Memb. Sci. 455 (2014) 254–270. https://doi.org/10.1016/j.memsci.2013.12.054.

[64] N.P. Berezina, S. V. Timofeev, N.A. Kononenko, Effect of conditioning techniques of perfluorinated sulphocationic membranes on their hydrophylic and electrotransport properties, J. Memb. Sci. 209 (2002) 509–518. https://doi.org/10.1016/S0376-7388(02)00368-X.

[65] N.D. Pismenskaya, E.E. Nevakshenova, V. V. Nikonenko, Using a Single Set of Structural and Kinetic Parameters of the Microheterogeneous Model to Describe the Sorption and Kinetic Properties of Ion-Exchange Membranes, Pet. Chem. 58 (2018) 465–473. https://doi.org/10.1134/S0965544118060087.

[66] R. Lteif, L. Dammak, C. Larchet, B. Auclair, Conductivité électrique membranaire: Étude de l'effet de la concentration, de la nature de l'electrolyte et de la structure membranaire, Eur. Polym. J. 35 (1999) 1187–1195. https://doi.org/10.1016/S0014-3057(98)00213-4.

[67] L.V. Karpenko, O.A. Demina, G.A. Dvorkina, S.B. Parshikov, C. Larchet, B. Auclair, N.P. Berezina, Comparative study of methods used for the determination of electroconductivity of ion-exchange membranes, Russ. J. Electrochem. 37 (2001) 287–293. https://doi.org/10.1023/A:1009081431563.

[68] V. Sarapulova, I. Shkorkina, S. Mareev, N. Pismenskaya, N. Kononenko, C. Larchet, L. Dammak, V. Nikonenko, Sarapulova, Shkorkina, Mareev, Pismenskaya, Kononenko, Larchet, Dammak, Nikonenko, V. Sarapulova, I. Shkorkina, S. Mareev, N. Pismenskaya, N. Kononenko, C. Larchet, L. Dammak, V. Nikonenko, Transport characteristics of fujifilm ion-exchange membranes as compared to homogeneous membranes AMX and CMX and to heterogeneous membranes MK-40 and MA-41, Membranes (Basel). 9 (2019). https://doi.org/10.3390/membranes9070084.

 doi:10.20944/preprints202205.0055.v1

[69] P.A. Sosa-Fernández, J.W. Post, H.L. Nabaala, H. Bruning, H. Rijnaarts, Experimental evaluation of anion exchange membranes for the desalination of (Waste) water produced after polymer-flooding, Membranes (Basel). 10 (2020) 1–22. https://doi.org/10.3390/membranes10110352.

[70] F.J. Danielli, D.A. Cadenhead, M.D. Rosenberg, Progress in surface and membrane science. Volume 7, Academic Press, 2016.

[71] A. Lévêque, Les lois de la transmission de chaleur par convection., Ann. Des Mines. 13 (1928) 201–299.

[72] V.I. Zabolotskii, N.V. Shel'deshov, N.P. Gnusin, Dissociation of Water Molecules in Systems with Ion-exchange Membranes, Russ. Chem. Rev. 57 (1988) 801–808. https://doi.org/10.1070/RC1988v057n08ABEH003389.

[73] J. Kamcev, D.R. Paul, B.D. Freeman, Ion activity coefficients in ion exchange polymers: Applicability of Manning's counterion condensation theory, Macromolecules. 48 (2015) 8011–8024. https://doi.org/10.1021/acs.macromol.5b01654.

[74] M.J.W. Frank, J.A.M. Kuipers, W.P.M. Van Swaaij, Diffusion coefficients and viscosities of CO2+H2O, CO2+CH3OH, NH3+H2O, and NH3+CH3OH liquid mixtures, 41 (1996) 297–302.